General Disclaimer

One or more of the Following Statements may affect this Document

- This document has been reproduced from the best copy furnished by the organizational source. It is being released in the interest of making available as much information as possible.

- This document may contain data, which exceeds the sheet parameters. It was furnished in this condition by the organizational source and is the best copy available.

- This document may contain tone-on-tone or color graphs, charts and/or pictures, which have been reproduced in black and white.

- This document is paginated as submitted by the original source.

- Portions of this document are not fully legible due to the historical nature of some of the material. However, it is the best reproduction available from the original submission.

Produced by the NASA Center for Aerospace Information (CASI)

NASA TECHNICAL
MEMORANDUM

NASA TM X-74000

A FOURTH-ORDER BOX METHOD FOR SOLVING

THE BOUNDARY-LAYER EQUATIONS

Stephen F. Wornom

January 1977

NATIONAL AERONAUTICS AND SPACE ADMINISTRATION

LANGLEY RESEARCH CENTER, HAMPTON, VIRGINIA 23665

1. Report No. NASA TM X-74000	2. Government Accession No.	3. Recipient's Catalog No.
4. Title and Subtitle A FOURTH-ORDER BOX METHOD FOR SOLVING THE BOUNDARY-LAYER EQUATIONS		5. Report Date January 1977
		6. Performing Organization Code
7. Author(s) Stephen F. Wornom		8. Performing Organization Report No.
9. Performing Organization Name and Address NASA Langley Research Center Hampton, Virginia 23665.		10. Work Unit No. 505-06-33-08-00
		11. Contract or Grant No.
12. Sponsoring Agency Name and Address National Aeronautics and Space Administration Washington, DC 20546		13. Type of Report and Period Covered NASA Technical Memorandum
		14. Sponsoring Agency Code

15. Supplementary Notes

Final release of information to be used as a reference for a formal publication

16. Abstract

A fourth-order box method for calculating high-accuracy numerical solutions to parabolic, partial differential equations in two variables or ordinary differential equations is presented. The method is the natural extension of the second-order Keller "Box" scheme to fourth order and is demonstrated with application to the incompressible, laminar and turbulent boundary-layer equations. Numerical results for high-accuracy test cases show the method to be significantly faster than other higher-order and second-order methods available today.

17. Key Words (Suggested by Author(s)) (STAR category underlined) Numerical analysis Boundary layers High accuracy solutions Boundary-value problems	18. Distribution Statement Unclassified-unlimited		
19. Security Classif. (of this report) Unclassified	20. Security Classif. (of this page) Unclassified	21. No. of Pages 25	22. Price* $3.50

A FOURTH-ORDER BOX METHOD FOR SOLVING
THE BOUNDARY-LAYER EQUATIONS

By Stephen F. Wornom

Langley Research Center

SUMMARY

A fourth-order box method for calculating high-accuracy numerical solutions to parabolic, partial differential equations in two variables or ordinary differential equations is presented. The method is the natural extension of the second-order Keller "Box" scheme to fourth order and is demonstrated with application to the incompressible, laminar and turbulent boundary-layer equations. Numerical results for high-accuracy test cases show the method to be significantly faster than other higher-order and second-order methods available today.

INTRODUCTION

Recently, attention has been given to numerical methods for solving the boundary-layer equations which have truncation errors that are of higher order than the second-order methods presently in use today. The term higher order will refer in this paper to the truncation error in the coordinate normal to the body surface. The truncation error in the tangential coordinate is second order. The advantages of higher-order methods are twofold. First, they can be used to obtain a numerical solution as accurate as a second-order method with considerably less computer time and storage or, alternatively, they may be used to produce a significantly more accurate solution for the same amount of run time and storage as a second-order method.

The higher-order methods proposed thus far for the boundary-layer equations consist of three-point schemes which fall into two classes. The first

class consists of collocation procedures which are fourth order for uniform meshes. These procedures treat the functional value and certain derivatives as unknowns at three collocation points and can be derived via Taylor Series (Hermite) or polynomial interpolation (Spline). In this category are the Padé approximation of Kreiss[1] or so-called compact scheme[2], the Mehrstellen[3] formulation, and the formulation of Peters[4]. The second class consists of methods for variable meshes. In this category are the Spline collocation methods of Rubin and Graves[5] and Rubin and Khosla[6,7]. Both classes are similar in that the resulting finite-difference equations involve three nodal points, but are different in that the first class is restricted to constant meshes whereas the second class is applicable to variable meshes.

One disadvantage of the higher-order methods involving three nodal points is that the usual boundary conditions for incompressible flow, $u = v = 0$ at the surface and $u \rightarrow u_e$ as the boundary layer merges with the the mainstream, are no longer sufficient since the resulting system of finite-difference equations contains two more unknowns than equations. This difficulty is usually finessed by adding an additional boundary condition at the outer edge of the layer and an additional equation or boundary condition at the surface boundary. The choice of which additional boundary conditions or equations to use is not clear.

Another disadvantage that is evident in some higher-order methods is the complexity of the resulting nonlinear finite-difference equations and the associated difficulty of solving them efficiently at each column. For example, the "Spline 4" method of Rubin and Khosla[6,7] would seem to require the solution of a 5X5-block tridiagonal matrix in order to solve the fully-coupled incompressible boundary-layer equations. A simpler solution scheme, which "lags" the continuity equation one iteration behind the momentum equation, is reported by Rubin and Khosla[6]. Since the equations in this scheme are solved uncoupled, the errors will diminish in a linear manner with each iteration. In contrast, the better second-order methods, such as the Davis Coupled Scheme[8] (DCS) or the Keller Box Scheme[9] (KBS), solve the equations fully coupled with Newton iteration and thus, for laminar flows, quadratic convergence is achieved. Hence, the advantages of some higher-order methods, relative to second-order methods, may be diminished or lost entirely in practical engineering calculations.

2

The purpose of this report is to present a fourth-order box method for obtaining numerical solutions to parabolic, partial-differential equations in two variables or ordinary differential equations, with application here to the steady, two-dimensional, incompressible, laminar or turbulent boundary-layer equations. The method has the following features: (1) The method results in finite-difference equations that involve only two nodal points and therefore is formally fourth-order accurate on all grids, (2) the method results in a 3X3 matrix of unknowns at each nodal point when the equations are solved in a coupled manner, (3) the method utilizes Newton iteration and demonstrates quadratic convergence for laminar flows, and (4) the method requires only the standard boundary conditions $u = v = 0$ at the body surface and $u \to u_e$ as the boundary layer merges with the mainstream. In short, the method is the natural fourth-order extension of the second-order Keller Box Scheme; it is an example of a general class of high-accuracy, two-point methods discussed briefly by Keller[10]. Keller offers an operation-count analysis that suggests that such methods may be superior to the well-known KBS (with Richardson extrapolation) to achieve accuracy less than or equal to $O(h^6)$. The validity of this conjecture is borne out in the present formulation and numerical results.

<div align="center">SYMBOLS</div>

A_n, B_n	3X3 matrices defined by equation (27)
a_{ij}	i,jth element of the A_n
b_{ij}	i,jth element of the B_n
C	3X3 matrix given by equation (31)
C_f	surface skin friction coefficient, $$C_f = \tau_w^* \Big/ \left(1/2 \; \rho_\infty^* U_\infty^{*2}\right)$$
$C_{f_{exact}}$	value of C_f for 640 intervals across the boundary layer

c_0, c_1	constants in grid stretch function - see equation (42)
D_n	3X3 matrix given by equation (37)
$d_n^{(1)}, d_n^{(2)}, d_n^{(3)}$ $e_n^{(1)}, e_n^{(2)}, e_n^{(3)}$	coefficients in the solution technique - see equations (32) to (34)
E_τ	percentage error in the wall shear - see equation (41)
F	damping factor - see equation (10c)
f	normalized longitudinal velocity component in the boundary layer $f = u/U_e$
g	represents any sufficiently differentiable quantity
h	step size in the η coordinate $h = \Delta\eta_{n-1} = \eta_n - \eta_{n-1}$
k	von Karman constant, $k = .41$
L^*	reference length
ℓ	$\ell = 1 + \varepsilon$
p_n, q_n, r_n	components of the vector $\vec{w}_n$ - see equation (26)
R_e	characteristic Reynolds number $R_e = \rho_\infty^* U_\infty^* L^* / \mu_\infty^*$
s	$\partial f/\partial \eta$
s_{exact}	value of s_1 (wall shear) for 640 intervals across the boundary layer

4

t	defined by equation (10b)
U	nondimensional inviscid flow velocity in the x-direction $U = U^*/U_\infty^*$
u	nondimensional time-averaged viscous flow component in the x-direction $u = \bar{u}^*/U_\infty^*$
u_τ^*	friction velocity $u_\tau^* = \sqrt{|\tau_w^*|/\rho_\infty^*}$
$\bar{v}$	nondimensional time-averaged viscous flow component in the Y-direction $\bar{v} = \sqrt{R_e}\ \bar{v}^*/U_\infty^*$
v	transformed viscous flow component in the y-direction - see equation (7)
$\vec{w}_n$	vector defined by equation (26)
x	nondimensional position coordinate measured along body surface from leading edge or stagnation point, $x = x^*/L^*$
Y	stretched normal coordinate $Y = \sqrt{R_e}\ y$
Y^+	law of the wall coordinate $Y^+ = u_\tau^* y^*/\nu_\infty^*$
y	nondimensional physical distance normal to body surface $y = y^*/L^*$
$\vec{z}_n$	vector defined by equation (25)
α	exponent in grid stretch function - see equation (42)
β	pressure gradient parameter - see equation (8)
$\Delta\eta$	step size in η coordinate $h = \Delta\eta_{n-1} = \eta_n - \eta_{n-1}$

5

$\bar{\delta}$ boundary-layer thickness measured in the η coordinate. Defined as the point where $u/U_e = .995$ unless otherwise noted

δ boundary-layer thickness measured in the Y coordinate

ε nondimensional eddy viscosity - see equation (10a)

ζ defined by equation (44)

η transformed normal coordinate - see equation (5)

λ mixing length - see equation (10d)

μ^* molecular viscosity

ν^* kinematic viscosity $\nu^* = \mu^*/\rho^*$

ξ transformed surface coordinate - see equation (5)

ρ^* density

τ_w^* wall shear $\tau_w^* = (\mu^* \partial u^*/\partial y^*)_{y=0}$

ϕ dummy integration variable - see equation (5)

ψ, ω coefficients used to compute s_1 - see equation (40)

6

Subscripts

e	inviscid flow conditions at $y = 0$
w	viscous flow conditions at $y = 0$
∞	free-stream conditions
n	grid index in η coordinate for finite-difference formulation
exact	value obtained with 640 intervals across boundary layer

Superscripts

i	present iteration
'	differentiation with respect to the η coordinate
—	time-averaged quantity
*	dimensional quantity
-1	inverse of matrix
→	vector
T	transpose of a matrix (or vector)
(1),(2), or (3)	coefficients associated with unknowns s, f, or v, respectively, in equations (32) to (39)

GOVERNING EQUATIONS

The method is demonstrated with application to the steady, two-dimensional, incompressible, laminar or time-averaged turbulent boundary-layer equations[11] which are expressed here in Görtler variables[12].

$$\frac{\partial}{\partial \eta}\left(\ell \frac{\partial f}{\partial \eta}\right) - v \frac{\partial f}{\partial \eta} - \beta(f^2 - 1) - 2\xi f \frac{\partial f}{\partial \xi} = 0 \qquad \text{(momentum)} \quad (1)$$

$$\frac{\partial v}{\partial \eta} + 2\xi \frac{\partial f}{\partial \xi} + f = 0 \qquad\qquad \text{(continuity)} \quad (2)$$

with boundary conditions

$$f = v = 0 \quad \text{at} \quad \eta = 0 \quad \text{(no slip, no injection)} \quad (3)$$

and

$$f \to 1 \quad \text{as} \quad \eta \to \infty. \tag{4}$$

Other quantities are given by

$$\xi = \int_0^x U_e(\phi)\, d\phi; \qquad \eta = \frac{U_e(x)}{\sqrt{2\xi}}\, Y, \tag{5}$$

$$f = u/U_e, \tag{6}$$

$$v = \frac{\sqrt{2\xi}}{U_e}\, \bar{v} + 2\xi\, f\, \frac{\partial \eta}{\partial x}\Big/ U_e, \tag{7}$$

$$\beta = \frac{2\xi}{U_e} \frac{dU_e}{d\xi}, \tag{8}$$

8

and

$$\ell = 1 + \epsilon. \tag{9}$$

The eddy viscosity ϵ is given by[13]

$$\epsilon = t \left| \frac{\partial \bar{\tau}}{\partial \eta} \right| \tag{10a}$$

where

$$t = F^2 \lambda^2 \sqrt{R_e} \, U_e^2 / \sqrt{2\xi} \tag{10b}$$

$$F = 1 - \exp\left(-Y^+/26\right) \tag{10c}$$

and

$$\frac{\lambda}{\delta} = .085 \, \tanh\left(\frac{k}{.085} \frac{Y}{\delta}\right) \qquad (k = .41) \tag{10d}$$

The variables in equations (1) to (10) are nondimensional as shown in the list of symbols.

FINITE-DIFFERENCE EQUATION FORMULATION

The usual approach for reducing a set of differential equations to a set of finite-difference equations is to express the partial derivative terms as finite-difference quotients and substitute those into the differential equations to obtain a set of finite-difference equations. Here we reverse the procedure and substitute the differential equations into a finite-difference expression to obtain a set of finite-difference equations.

9

The finite-difference expression around which the method is formulated is given by

$$g_n - g_{n-1} - \frac{h}{2}\left(g_n' + g_{n-1}'\right) + \frac{h^2}{12}\left(g_n'' - g_{n-1}''\right) + O(h^5) = 0 \tag{11}$$

where h is the variable step size, $\eta_n - \eta_{n-1}$, in the normal coordinate η and $(\ )' \equiv \partial(\ )/\partial\eta$ with g representing any sufficiently differentiable quantity. As mentioned previously, equation (11) is not new. It is the fourth-order member of a general class of high-accuracy, two-point methods for boundary-value problems discussed by Keller[10]. Liniger and Willoughby[14] analyzed the stability of equation (11) as an implicit method for solving initial-value problems for stiff systems of ordinary differential equations. Hirsh[2] used the expression to formulate boundary conditions for the three-point "compact" scheme applied to the incompressible driven cavity problem.

A key step in the present procedure, as with the second-order Keller Box Scheme, is to reformulate the problem in terms of a first-order set of partial differential equations. This is done by defining $s \equiv \partial f/\partial\eta$ and rewriting equations (1) and (2) as

$$\frac{\partial}{\partial\eta}(\ell s - vf) = 2\xi\frac{\partial f^2}{\partial\xi} + (1 + \beta)\ f^2 - \beta \qquad \text{(momentum)} \tag{12}$$

$$\frac{\partial f}{\partial\eta} = s \qquad \text{(shear)} \tag{13}$$

$$\frac{\partial v}{\partial\eta} = -2\xi\frac{\partial f}{\partial\xi} - f. \qquad \text{(continuity)} \tag{14}$$

If we now define g as a vector

$$\vec{g} = \left\{ \begin{array}{c} \ell s - vf \\ f \\ v \end{array} \right\} \qquad \begin{array}{c} (15) \\ (16) \\ (17) \end{array}$$

10

then $\vec{g}'$ will be the right-hand side of equations (12) to (14) and $\vec{g}''$ its derivative with respect to the η coordinate, as follows:

$$\vec{g}' = \begin{cases} 2\xi \dfrac{\partial f^2}{\partial \xi} + (1 + \beta)\, f^2 - \beta & (18) \\[2mm] s & (19) \\[2mm] -\, 2\xi \dfrac{\partial f}{\partial \xi} - f & (20) \end{cases}$$

$$\vec{g}'' = \begin{cases} 2\left[2\xi \dfrac{\partial (fs)}{\partial \xi} + (1 + \beta)\,(fs) \right] & (21) \\[2mm] (2\ell - 1)^{-1}\left[vs + \beta(f^2 - 1) + \xi \dfrac{\partial f^2}{\partial \xi} - t'\,|s|s \right] & (22) \\[2mm] -\, 2\xi \dfrac{\partial s}{\partial \xi} - s & (23) \end{cases}$$

where equation (1) has been used to express s' in terms of the dependent variables f, s, and v (eq. (22)). Substitution of equations (15) to (23) into equation (11) leads to three nonlinear finite-difference equations. The $\partial(\ )/\partial \xi$ terms in these equations are written so as to handle either the Crank-Nicolson scheme, where they are approximated by a central difference quotient, or a scheme where they are approximated by three points; thus in either case making the equations second-order accurate in the ξ coordinate and fourth-order accurate in the normal coordinate η. These nonlinear equations are then linearized by Newton's method with the exception of the term $t'|s|s$ in equation (22) and the quantities δ and s_1 which are used to compute λ and Y^+.

Application of Newton's method yields three linear finite-difference equations which can be expressed as

$$A_n \vec{z}_{n-1} + B_n \vec{z}_n = \vec{w}_n \tag{24}$$

11

where

$$\vec{z}_n = (s_n^i, f_n^i, v_n^i)^T \tag{25}$$

$$\vec{w}_n = (p_n, q_n, r_n)^T \tag{26}$$

$$A_n = \begin{bmatrix} a_{11} & a_{12} & a_{13} \\ a_{21} & a_{22} & a_{23} \\ a_{31} & a_{32} & a_{33} \end{bmatrix} \quad B_n = \begin{bmatrix} b_{11} & b_{12} & b_{13} \\ b_{21} & b_{22} & b_{23} \\ b_{31} & b_{32} & b_{33} \end{bmatrix} \tag{27}$$

The superscript i in equation (25) denotes the present iteration value. A_n, B_n, and $\vec{w}_n$ are functions of the dependent variables evaluated at the $i-1$ iteration and/or at the previous ξ stations. Equations (24) must be solved repeatedly until an acceptable level of convergence is obtained. Although the double-subscripted matrix elements change values with the index n, the index n is suppressed here for simplicity. The superscript i will be suppressed from here on for the same reason. Appendix A shows how a_{21}, a_{22}, a_{23}, b_{21}, b_{22}, b_{23}, and q_n are obtained.

The boundary conditions are

$$f_1 = v_1 = 0 \qquad \text{(No slip, no injection)} \tag{28}$$

and

$$f_N = 1 \tag{29}$$

It is noteworthy that, since equations (24) can be applied at the outer boundary, the total number of finite-difference equations available exactly balances the total number of unknowns. In contrast, a three-point method formulated in terms of f, s, and v (since it could not be applied at the outer boundary) would result in more unknowns than equations and hence the

12

method would require additional boundary conditions or use of three-point backward differencing at the outer boundary or a combination of both.

The resulting linear system of finite-difference equations (24) can be solved in the relatively simple manner which is presented here.

If equations (24) are applied at $n = 2$ ($n = 1$ being the surface and $n = N$ locating the outer boundary) and the boundary conditions $f_1 = v_1 = 0$ are applied, three equations with four unknowns are obtained. Thus, we may solve for three of the unknowns in terms of the fourth unknown.

Since f_N is known at the outer boundary, it is convenient to solve for s_1, s_2, and v_2 in terms of f_2, in anticipation of the general form of the recursion relations to be derived subsequently. Thus, at $n = 2$, equations (24) can be rewritten as:

$$(s_2, s_1, v_2)^T = C^{-1} \left[\vec{w}_2 - (b_{12}, b_{22}, b_{32})^T f_2 \right] \tag{30}$$

where

$$C = \begin{bmatrix} b_{11} & a_{11} & b_{13} \\ b_{21} & a_{21} & b_{23} \\ b_{31} & a_{31} & b_{33} \end{bmatrix} \tag{31}$$

.If we next apply equations (24) at $n = 3$ and use equations (30) to eliminate s_2 and v_2 as unknowns, the result is again three equations and four unknowns; namely, f_2, f_3, v_3, and s_3. Thus, we may solve for three of the unknowns in terms of the fourth unknown. Here we solve for f_2, v_3, s_3, in terms of f_3; this order being dictated by the choice at $n = 2$ which was made with the consideration of the outer boundary condition $f_N = 1$. If this procedure is repeated for $n = 4, \ldots, N$, the following general form is obtained for the three unknowns written in terms of the fourth:

$$s_n = d_n^{(1)} + e_n^{(1)} f_n \tag{32}$$

$$f_{n-1} = d_n^{(2)} + e_n^{(2)} f_{ii} \qquad\qquad n = 3, 4, \ldots, N. \tag{33}$$

$$v_n = d_n^{(3)} + e_n^{(3)} f_n \tag{34}$$

where the superscripts 1, 2, and 3 in parentheses identify the coefficients associated with the unknowns s, f, and v, respectively.

The coefficients $d_n^{(1)}$, $d_n^{(2)}$, $d_n^{(3)}$, $e_n^{(1)}$, $e_n^{(2)}$, and $e_n^{(3)}$ are given by

$$\left(d_n^{(1)}, d_n^{(2)} d_n^{(3)} \right)^T = D_n^{-1} \left[(p_n, q_n, r_n)^T - (a_{11}, a_{21}, a_{31})^T d_{n-1}^{(1)} \right.$$
$$\left. - (a_{13}, a_{23}, a_{33})^T d_{n-1}^{(3)} \right] \tag{35}$$

$$\left(e_n^{(1)}, e_n^{(2)}, e_n^{(3)} \right)^T = - D_n^{-1} (b_{12}, b_{22}, b_{32})^T \tag{36}$$

with

$$D_n = \begin{bmatrix} b_{11} & a_{12} + a_{11} e_{n-1}^{(1)} + a_{13} e_{n-1}^{(3)} & b_{13} \\ b_{21} & a_{22} + a_{21} e_{n-1}^{(1)} + a_{23} e_{n-1}^{(3)} & b_{23} \\ b_{31} & a_{32} + a_{31} e_{n-1}^{(1)} + a_{33} e_{n-1}^{(\cdot)} & b_{33} \end{bmatrix} \tag{37}$$

14

Examination of equations (32) to (37) reveals that while the solution for the dependent variables s_n, f_n, and v_n cannot be computed as we proceed toward the outer boundary, the coefficients $d_n^{(1)}$, $d_n^{(2)}$, $d_n^{(3)}$, $e_n^{(1)}$, $e_n^{(2)}$, and $e_n^{(3)}$ can be computed if the initial values $d_2^{(1)}$, $d_2^{(3)}$, $e_2^{(1)}$, and $e_2^{(3)}$ are known. These initial values are found by comparing equations (32) and (34) evaluated at $n = 2$ with equations (30). The initial values are:

$$\left(d_2^{(1)}, \psi, d_2^{(3)} \right)^T = C^{-1} (p_2, q_2, r_2)^T \tag{38}$$

$$\left(e_2^{(1)}, \omega, e_2^{(3)} \right)^T = - C^{-1} (b_{12}, b_{22}, b_{32})^T \tag{39}$$

where ψ, ω are coefficients to compute s_1 from the following equation

$$s_1 = \psi + \omega f_2. \tag{40}$$

When the outer boundary is reached, equations (32) to (34) can now be solved for s_N, f_{N-1}, and v_N since the outer boundary condition $f_N = 1$ can be applied. Knowing f_{N-1}, we can next compute s_{N-1}, f_{N-2}, and v_{N-1} and likewise all the values of s_n, f_n, and v_n proceeding from the outer boundary toward the solid boundary.

RESULTS AND DISCUSSION

Figure 1 shows the percent error in the wall shear versus the number of intervals across the boundary layer, N-1, for the present method, the Spline 4 method of Rubin and Khosla[6] and the KBS for stagnation point flow ($\beta = 1$). The number of intervals were 5, 10, 16, 20, 32, 40, 64, 80, 128, 160, and 320. The Spline 4 method was unstable for five intervals and thus no point is shown. For

this case the governing equations reduce to a set of ordinary differential equations. The error in the wall shear is defined as

$$E_\tau = 100 \, |s_{exact} - s_1| / s_{exact} \tag{41}$$

where s_{exact} is the value of s_1 from the higher-order methods with 640 intervals across the boundary layer. The mesh size for this case varied across the layer (e.g., $\Delta\eta_1 = .05$ for $N = 11$) with the last computational point being at $\eta_N = 24.2538$. The equation used to generate the grid is given by

$$\eta_n = c_0 \, \zeta_n / (1 + c_1 \zeta_n)^\alpha, \tag{42}$$

where

$$c_0 = \eta_N \, (1 + c_1)^\alpha \tag{43}$$

$$\zeta_n = (n-1)/(N-1), \tag{44}$$

and

$$c_1 = -.4, \, \alpha = 8.26 \tag{45}$$

The two extra equations needed for the Spline 4 method were taken as

$$s_N = 0 \tag{46}$$

and equation (11) applied at $n = 2$ to the shear equation.

Figure 1 shows both the present method and the Spline 4 method of Rubin and Khosla[6] to be fourth-order accurate for a variable mesh. However, for the same number of nodal points across the boundary layer, the present method

16

is approximately 10 times as accurate as the Spline 4 method for a variable mesh size. To judge the efficiency of the different higher-order methods, the computer run times for the different methods were compared for three high-accuracy solutions to this problem; namely, E_τ = .15, .015, and .0015. To achieve an error of E_τ = .15 the present method, the Spline 4 method, and the KBS solutions were computed with 7, 11, and 27 nodal points, respectively. (See fig. 1.) The convergence criteria for these three cases required the value of E_τ between consecutive iterations to be accurate to two significant figures. Results are summarized in tables I, II, and III. These tables show the present method to be significantly faster than the Spline 4 and the KBS to achieve the same degree of accuracy. It should be noted that a key reason for the greater efficiency of the present method over the Spline 4 method is due to the present equation formulation which allows the resulting finite-difference equations to be solved efficiently in a coupled manner using Newton's method.

Figure 2 shows a plot of the percentage error in the wall shear versus the number of intervals across the boundary layer for a model turbulent problem for the present method and the KBS. The equations for this case were obtained from the nonsimilar equations by setting β = 0 and $\partial(\ )/\partial\xi$ = 0. The Reynolds number was 1.88 million, ξ = 1, $\bar{\delta}$ = 24.5 with the outer boundary located at η_N = 60. Convergent solutions using the Spline 4 could not be obtained for this case. (The possibility of a coding error exists in the program and this will be investigated further.) The constants in equation (42) for the η grid distribution are c_1 = .05 and α = -109. Figure 2 shows the present method to be slightly better than third-order accurate for the model turbulent problem. In order to determine the efficiency of the present method, solutions were computed with both methods for a .1-percent error in the wall shear. The present method requires approximately 21 nodal points and the KBS 92 nodal points. Results show the present method to be approximately 3.83 times faster than the KBS to achieve the same order of accuracy. All calculations were made on a CDC Cyber 175 computer with a FORTRAN Extended Compiler, optimization level = 0. The same calculations would require about 2.5 times more CPU time on a CDC 6600. No under-relaxation was required for either test case.

17

CONCLUDING REMARKS

A fourth-order box method for calculating high-accuracy numerical solu-
tions to parabolic, partial differential equations in two variables or ordinary
differential equations has been presented. The method is the natural extension
of the second-order Keller "Box" scheme to fourth order and has been demon-
strated with application to the incompressible, laminar and turbulent boundary-
layer equations. Numerical results for high accuracy test cases show the
present method to be significantly faster than other higher-order and second-
order methods available today to achieve the same accuracy. For the test
cases reported on the governing equations reduced to ordinary differential
equations. Calculations for nonsimilar cases have been completed and will
be included in a later report.

Richardson extrapolation to zero mesh size has not been considered in
the present paper. Keller has shown this technique to be a valuable one
for improving the accuracy of the KBS; hence, a final comparison must be
made on this basis.

18

REFERENCES

1. Orszag, S. A.; and Israeli, M.: Numerical Simulation of Viscous In-
   compressible Flows. Annual Review of Fluid Mechanics, Annual Reviews,
   Inc., Palo Alto, 1974.

2. Hirsh, R.: Higher Order Accurate Difference Solutions of Fluid Mechanics
   Problems by a Compact Differencing Technique. J. Comp. Phys., $\underline{19}$, 1,
   pp. 90-109, September 1975.

3. Krause, E.; Hirschel, E. H.; and Kordulla, W.: Fourth Order "Mehrstellen"-
   Integration for Three Dimensional Turbulent Boundary Layers. Proc. of
   AIAA Computational Fluid Dynamics Conference, Palm Springs, Calif.,
   pp. 92-102, July 1973.

4. Peters, N.: Boundary Layer Calculation by an Hermitian Finite Difference
   Method. Fourth International Conference on Numerical Methods in Fluid
   Mechanics, Boulder, Colo., June 1974.

5. Rubin, S. G.; and Graves, R. A.: Viscous Flow Solutions With a Cubic
   Spline Approximation. Computers and Fluids, $\underline{3}$, 1, pp. 1-36, 1975.
   See also NASA TR R-436, 1975.

6. Rubin, S. G.; and Khosla, P. K.: Higher-Order Numerical Solutions Using
   Cubic Splines. Proc. of AIAA Second Computational Fluid Dynamics Con-
   ference, Hartford, Conn., pp. 55-66, June 1975. See also NASA CR-2653,
   February 1976.

7. Rubin, S. G.; and Khosla, P. K.: Higher-Order Numerical Methods Derived
   From Three-Point Polynomial Interpolation. NASA CR-2735, August 1976.

8. Blottner, F. G.: Investigation of Some Finite-Difference Techniques for
   Solving the Boundary Layer Equations. Computer Methods in Applied
   Mechanics and Engineering, vol. 6, pp. 1-30, 1975.

9. Keller, H. B.: A New Difference Scheme for Parabolic Problems. Numerical
   Solution of Partial Differential Equations, vol. II, edited by J. Bramble,
   Academic Press, New York, 1970.

10. Keller, H. B.: Numerical Solution of Boundary Value Problems for Ordinary
    Differential Equations: Survey and Some Recent Results on Difference
    Methods. Numerical Solutions of Boundary Value Problems for Ordinary
    Differential Equations, A. K. Aziz, ed., Academic Press, New York,
    pp. 27-88, 1975.

11. Schlichting, H.: Boundary-Layer Theory. McGraw-Hill Book Company,
    Sixth Edition, p. 545, 1968.

12. Görtler, H.: A New Series for the Calculation of Steady Laminar Boundary Layer Flows. J. Math. and Mech., vol. 6, pp. 1-66, January 1957.

13. Michel, R.; Quemard, C.; and Durant, R.: Hypotheses on the Mixing Length and Application to the Calculation of the Turbulent Boundary Layers. Proceedings of Computation of Turbulent Boundary Layers - 1968 AFOSR-IFP - Stanford Conference, vol. 1, pp. 195-212.

14. Liniger, W.; and Willoughby, R. A.: Efficient Integration Methods for Stiff Systems of Ordinary Differential Equations. SIAM J. Numer. Anal. 7, pp. 47-66, 1970.

20

APPENDIX A

SHEAR EQUATION COEFFICIENTS

We show here how to identify the matrix elements of A_n, B_n and the vector component of $\vec{w}_n$ for equations (24). The procedure is illustrated for the shear equation for laminar, similar flow ($\ell = 1$, $\partial(\ )/\partial\xi = 0$) where for the shear equation

$$g = f \tag{A1}$$

$$g' = s \tag{A2}$$

$$g'' = s' = vs + \beta (f^2 - 1). \tag{A3}$$

Substitution of equations (A1) to (A3) into equation (11) evaluated at the ith iteration yields the following nonlinear finite-difference equation

$$f_n^i - f_{n-1}^i - \frac{h}{2}\left(s_n^i + s_{n-1}^i\right) + \frac{h^2}{12}\left[(vs)_n^i + \beta\left\{(f^2)_n^i - 1\right\}\right.$$

$$\left. - (vs)_{n-1}^i - \beta\left\{(f^2)_{n-1}^i - 1\right\}\right] = 0 \tag{A4}$$

Equation (A4) is now linearized via Newton's method which can be shown to correspond to the following linearization for the products $(vs)^i$ and $(f^2)^i$:

$$(vs)^i = v^{i-1}s^i + v^i s^{i-1} - (vs)^{i-1} \tag{A5}$$

21

$$(f^2)^i = 2f^{i-1}f^i - (f^2)^{i-1} \tag{A6}$$

Applying equations (A5) and (A6) to equation (A4), the linear finite-difference equation can be written as

$$a_{21}s_{n-1}^i + a_{22}f_{n-1}^i + a_{23}v_{n-1}^i + b_{21}s_n^i + b_{22}f_n^i + b_{23}v_n^i = q_n \tag{A7}$$

where

$$a_{21} = -h/2 - \frac{h^2}{12}v_{n-1}^{i-1} \tag{A8}$$

$$a_{22} = -1 - \frac{\beta h^2}{6}f_{n-1}^{i-1} \tag{A9}$$

$$a_{23} = -\frac{h^2}{12}s_{n-1}^{i-1} \tag{A10}$$

$$b_{21} = -\frac{h}{2} + \frac{h^2}{12}v_n^{i-1} \tag{A11}$$

$$b_{22} = 1 + \frac{\beta h^2}{6}f_n^{i-1} \tag{A12}$$

$$b_{23} = \frac{h^2}{12}s_n^{i-1} \tag{A13}$$

and

$$q_n = \frac{h^2}{12}\left[(vs)_n^{i-1} - (vs)_{n-1}^{i-1} + \beta\left\{(f^2)_n^{i-1} - (f^2)_{n-1}^{i-1}\right\}\right] \tag{A14}$$

22

TABLE I.- E_τ = .15 PERCENT (ERROR IN WALL SHEAR)

Method	Mesh Points	Iterations	CPU (a)	CPU/CPU$_{KBS}$
Present	7	3	0.008	0.53
Spline 4	11	11	0.033	2.2
KBS	27	3	0.015	1.0

[a] CPU = Central processing time in seconds.

TABLE II.- E_τ = .015 PERCENT (ERROR IN WALL SHEAR)

Method	Mesh Points	Iterations	CPU	CPU/CPU$_{KBS}$
Present	11	3	0.011	0.26
Spline 4	18	10	0.042	1.05
KBS	81	3	0.040	1.0

TABLE III.- E_τ = .0015 PERCENT (ERROR IN WALL SHEAR)

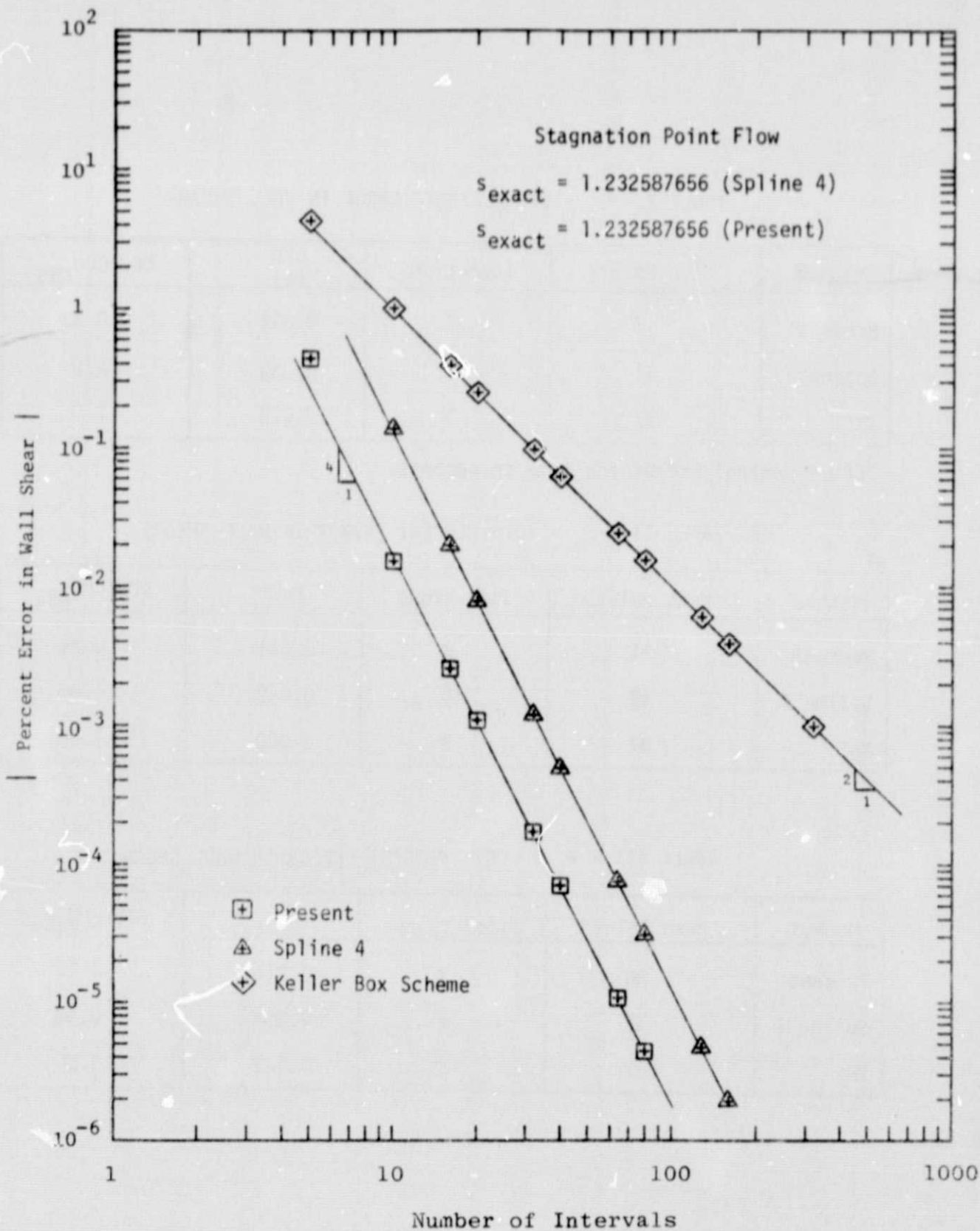| Method	Mesh Points	Iterations	CPU	CPU/CPU$_{KBS}$
Present	20	3	0.015	0.12
Spline 4	31	9	0.058	0.48
KBS	261	3	0.122	1.0

Figure 1.- Percent error in the wall shear versus the number of intervals across the boundary layer.
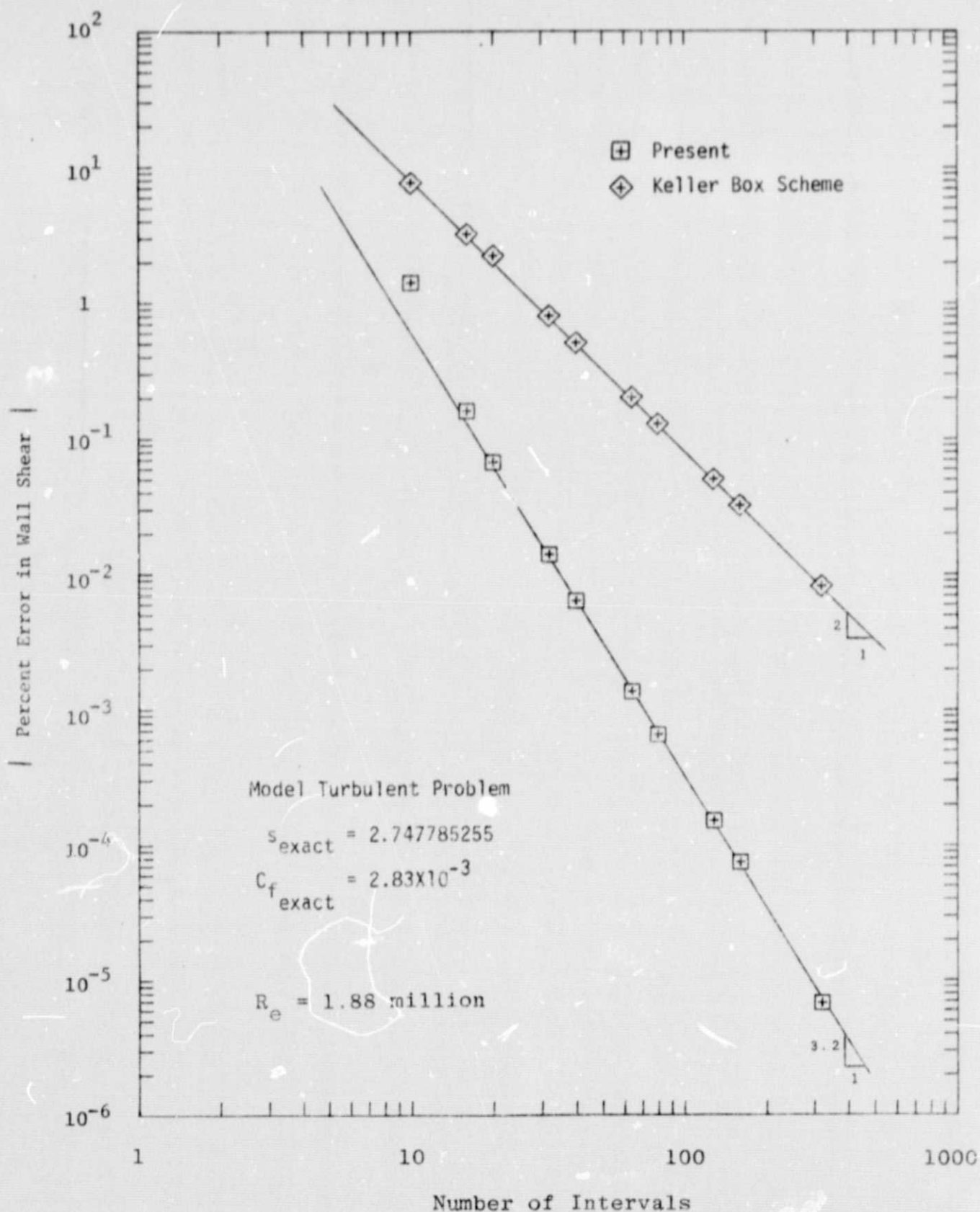
Figure 2.- Percent error in the wall shear versus the number of intervals across the boundary layer.